Brain Structure and Function (2021) 226:889–900
https://doi.org/10.1007/s00429-021-02216-9

ORIGINAL ARTICLE

Development of γ-aminobutyric acid-, glycine-, and glutamate-immunopositive boutons on the rat genioglossal motoneurons

Sang Kyoo Paik[1] · **Atsushi Yoshida**[2] · **Yong Chul Bae**[1]

Received: 5 August 2020 / Accepted: 8 January 2021 / Published online: 21 January 2021

Abstract

Detailed information about the development of excitatory and inhibitory synapses on the genioglossal (GG) motoneuron may help to understand the mechanism of fine control of GG motoneuron firing and the coordinated tongue movement during postnatal development. For this, we investigated the development of γ-aminobutyric acid (GABA)-immunopositive (GABA +), glycine + (Gly +), and glutamate + (Glut +) axon terminals (boutons) on the somata of rat GG motoneurons at a postnatal day 2 (P2), P6 and P18 by retrograde labeling of GG motoneurons with horseradish peroxidase, electron microscopic postembedding immunogold staining with GABA, Gly, and Glut antisera, and quantitative analysis. The number of boutons per GG motoneuron somata and the mean length of bouton apposition, measures of bouton size and synaptic covering percentage, were significantly increased from P2/P6 to P18. The number and fraction of GABA + only boutons of all boutons decreased significantly, whereas those of Gly + only boutons increased significantly from P2/P6 to P18, suggesting developmental switch from GABAergic to glycinergic synaptic transmission. The fraction of mixed GABA +/Gly + boutons of all boutons was the highest among inhibitory bouton types throughout the postnatal development. The fractions of excitatory and inhibitory boutons of all boutons remained unchanged during postnatal development. These findings reveal a distinct developmental pattern of inhibitory synapses on the GG motoneurons different from that on spinal or trigeminal motoneurons, which may have an important role in the regulation of the precise and coordinated movements of the tongue during the maturation of the oral motor system.

Keywords Hypoglossal motoneuron · Excitatory · Inhibitory · Presynaptic axon terminal · Development · Electron microscopy

Introduction

The precise pattern of excitatory and inhibitory synaptic inputs to the hypoglossal (HG) motoneurons encodes the timing of their motor output and, thus, plays a crucial role in the precise and coordinated tongue movement during oral behaviors, including respiration, chewing, sucking, and swallowing (Liu et al. 2003; Horner 2009). A subset of HG motoneurons, the genioglossal (GG) motoneurons, which innervate the primary tongue protrusor muscle genioglossus, are also involved in the maintenance of the upper airway patency during inspiration (Plowman et al. 1990).

Multiple authors have reported that the properties of the inhibitory and excitatory synapses onto the HG motoneuron change during postnatal development (Singer and Berger 2000; Carrascal et al. 2005; Berger 2011). For example, the inhibitory synaptic transmission changes from GABAergic to glycinergic during postnatal development (Muller et al. 2006; Gao et al. 2011). The expression, subunit composition and channel properties of the glycine receptor (GlyR) and the $GABA_AR$ receptor in the HG motoneurons also change during postnatal development (Singer and Berger 2000; Berger 2011; Muller et al. 2004, 2006). However, since the number and properties of the inhibitory synapses differ between the subregions of the hypoglossal nucleus (O'Brien

✉ Yong Chul Bae
ycbae@knu.ac.kr

[1] Department of Anatomy and Neurobiology, School of Dentistry, Kyungpook National University, 188-1, 2-Ga, Samdeok-Dong, Jung-Gu, Daegu 700-412, Korea

[2] Department of Oral Anatomy and Neurobiology, Graduate School of Dentistry, Osaka University, Osaka 565-0871, Japan

and Berger 2001), and most of the above studies were performed on non-specific HG motoneurons which were not identified for their innervating tongue muscles, the interpretability of their results is limited.

Information about the development of excitatory and inhibitory synapses on identified GG motoneurons may help to elucidate the mechanism underlying the fine control of GG motoneuron excitability, and hence the precise movement of the tongue during maturation of the oral motor function. Recently, we reported a distinct distribution pattern of excitatory and inhibitory synapses on the GG motoneurons (Paik et al. 2019). As a follow-up, we here investigated the distribution of excitatory and inhibitory synapses on the rat GG motoneurons during postnatal development by retrograde tracing of horseradish peroxidase, electron microscopic postembedding immunogold staining using antisera against γ-amino butyric acid (GABA), glycine (Gly) and glutamate (Glut), and quantitative analysis.

Materials and methods

All experimental procedures were performed with the explicit approval by the Kyungpook National University Intramural Animal Care and Use Committee.

Labeling of genioglossal motoneurons

Three male Sprague–Dawley rats at each of postnatal days 2 (P2), P6 and P18 were anesthetized with sodium pentobarbital (40 mg/kg, i.p.). An incision was made on the skin of the neck, and the digastric, mylohyoid, and geniohyoid muscles were spread apart to expose the genioglossus muscle. A total of three–five µl of 10% horseradish peroxidase (HRP, type IV, Toyobo, Japan; in normal saline) was injected into multiple sites on the right genioglossus muscle with a 30 G needle glued to a Hamilton micro-syringe. After 20–24 h, the rats were anesthetized with sodium pentobarbital (80 mg/kg, i.p.) and perfused transcardially with 100 ml of heparinized normal saline, followed by 500 ml of fixative containing 2.5% glutaraldehyde, 1% paraformaldehyde, and 0.1% picric acid in phosphate buffer (PB; 0.1 M, pH 7.4).

Tissue preparation

The brainstem was removed, post-fixed in the same fixative for 2 h at 4 °C, and stored in PB. Sixty-µm-thick serial transverse sections were prepared with a Vibratome. Retrogradely transported HRP was visualized according to the tungstate/tetramethylbenzidine protocol and further treated with 0.25 mg/ml diaminobenzidine in PB, as previously described (Weinberg and Eyck 1991; Park et al. 2018,2019a). Wet sections were examined under a light microscope, and sections containing multiple HRP-labeled neurons in the hypoglossal nucleus were selected, post-fixed with 0.5% osmium tetroxide in PB (pH 6.0) for 40 min, dehydrated in graded alcohols, flat-embedded in Durcupan ACM (Fluka, Switzerland), and cured for 48 h at 60 °C. Light micrographs (400×) of the HRP-labeled GG motoneurons at each developmental age were captured with a digital camera attached to the Zeiss Axioplan 2 microscope, and saved as TIFF files. The cross-sectional areas of the somata of the HRP-labeled motoneurons in a plane where the nucleolus is prominent were measured using a digitizing tablet and Image J software (NIH, Bethesda, MD).

Chips containing HRP-labeled GG motoneurons with prominent nucleoli were cut and glued onto blank blocks with cyanoacrylate. Serial thin sections were collected on formvar-coated single slot nickel grids. Grids were examined on Hitach H-7500 electron microscope (Hitachi, Tokyo, Japan) at 80 kV accelerating voltage. Electron micrographs were acquired by a cooled CCD camera (SC1000 Orius; Gatan, Pleasanton, CA, USA) attached to the electron microscope and saved as TIFF files. The brightness and contrast of the images were adjusted in Adobe Photoshop 7.0 (Adobe systems Inc., San Jose, CA).

Postembedding immunogold staining for GABA, glycine, and glutamate

Postembedding immunogold labeling for GABA, Gly, and Glut was performed as previously described (Paik et al. 2019; Bae et al. 2018; Park et al. 2019b). Briefly, the grids were treated for 10 min in 1% periodic acid and for 15 min in 9% sodium periodate. Sections were washed in distilled water, transferred to tris-buffered saline containing 0.1% triton X-100 (TBST; pH 7.4) for 10 min, and incubated in 2% human serum albumin (HAS, in TBST) for 10 min. The grids were further incubated with anti-GABA (GABA 990, 1:800), anti-Gly (glycine 290, 1:280), and anti-Glut (Glut 607, 1:1000) antisera. To eliminate cross reactivity, the antisera were pre-adsorbed overnight with glutaraldehyde-conjugated amino acids as previously described (Paik et al. 2019; Ottersen et al. 1986). After extensive rinse in TBST, grids were incubated for 3 h in goat anti-rabbit IgG coupled to 15-nm gold particles (1:25 in TBST). After rinse in distilled water, the grids were stained with uranyl acetate and lead citrate.

The antisera (a kind gift from Dr. Ottersen at the Centre for Molecular Biology and Neuroscience, University of Oslo, Norway) were raised against GABA, Gly or Glut conjugated to bovine serum albumin with glutaraldehyde and formaldehyde (Kolston et al. 1992; Broman et al. 1993). They were characterized by spot-testing (Ottersen and Storm-Mathisen 1984) and have been used routinely in our previous work (Paik et al. 2019; Bae et al. 2018;

Park et al. 2019b). Omission of the primary antisera or replacement with normal rabbit serum or preadsorption of the diluted anti-GABA serum with 200 µM GABA-G, the anti-Gly serum with 300 µM Gly-G, and the anti-Glut serum with 300 µM Glut-G, also abolished the specific immunostaining.

Quantitative analysis

Twelve, 10, and 13 GG motoneurons from P2, P6, and P18 rats, respectively, with larger than the average size somata in each of the age groups (> 400 µm^2 in cross-sectional area for P2, > 500 µm^2 for P6, > 650 µm^2 for P18) were selected for electron microscopic analysis. Electrophysiological studies reported that rat hypoglossal motoneurons mature and their inhibitory synaptic transmission changes greatly during the first 3 postnatal weeks (Singer and Berger 2000; Berger 2011). Thus, we analyzed GG motoneurons at neonatal (P2), intermediate (P6) and juvenile (P18) stages. Electron micrographs (25,000×) were taken along the entire somatic membrane in series of thin sections incubated with GABA, Gly and Glut antisera. To assess the immunoreactivity for GABA and Gly, we compared the density of gold particles within the immunoreactive boutons with that of their postsynaptic somata (background density). Boutons were considered immunopositive if the gold particle density over the vesicle-containing areas of the boutons was at least five times higher than the particle density in the corresponding postsynaptic region [this standard is used routinely for distinguishing the metabolic from the transmitter GABA and Gly in axon terminals; (Paik et al. 2019; Park et al. 2019b)]. To assess the immunoreactivity for Glut, gold particle density of each bouton was compared with the average tissue density in 10–15 randomly-selected areas adjacent to the somata of genioglossal motoneurons (2 µm^2 each, a total area of 20–30 µm^2 per section). Boutons containing gold particles at a density > average tissue density + 2.576 standard deviation (SD, significant difference at 99% confidence level) were considered Glut-immunopositive (Paik et al. 2019; Park et al. 2016). Measurements were performed on electron micrographs using a digitizing tablet and Image J software.

The following parameters were recorded for each somata: (1) perimeter and number of boutons apposing the somatic membrane, (2) mean length of bouton apposition, (3) fraction of somatic membrane covered by boutons (synaptic covering percentage), (4) number of boutons per 100 µm^2 of somatic membrane surface area (packing density). Statistical analysis for differences among each age groups was performed by analysis of variance (ANOVA); mean values were compared using Scheffe's F test. Significance was set at $p < 0.05$.

Results

GG motoneurons during postnatal development

At light microscopic examination, HRP-labeled GG motoneurons were observed in the ventral and ventrolateral subdivisions of the hypoglossal nucleus (Fig. 1). The size distribution of the HRP-labeled GG motoneurons during postnatal development is summarized in Fig. 2. The average size of the GG motoneuron somata increased significantly from P2 to P18 (cross-sectional area, mean ± SD: 362.0 ± 77.5 µm^2 at P2, 491.1 ± 112.1 µm^2 at P6, 619.6 ± 167.4 µm^2 at P18, $p = 0.0000$).

Presynaptic boutons on the GG motoneurons during postnatal development

At electron microscopic examination, the somata of the GG motoneurons, identified by the presence of retrogradely transported HRP in the cytoplasm (Fig. 1), were contacted by numerous boutons. A total of 188, 185, and 391 of these boutons on 12 somata in P2, 10 somata in P6, and 13 somata in P18, respectively, were analyzed (Table 1). The number of boutons per GG motoneuron somata, the mean length of boutons apposition (reflecting the bouton size and synaptic strength), and the synaptic covering percentage (the fraction of somatic membrane covered by boutons) were significantly higher from P2/P6 to P18. The packing density (number of boutons per 100 µm^2 somatic membrane) was unchanged between the three postnatal stages. No degenerative changes of boutons, such as darkening of the axoplasm or clumping of the synaptic vesicles were observed.

GABA +, Gly +, and Glut + boutons on the GG motoneurons during postnatal development

Based on the immunogold staining for GABA, Gly, and Glut on serial thin sections, the boutons apposing somata of GG motoneurons could be categorized as (1) immunopositive for GABA only (GABA + only, Figs. 3a–c and 5c, d), (2) immunopositive for Gly only (Gly + only, Fig. 5a, b), (3) immunopositive for both GABA and Gly (mixed GABA +/Gly +, Figs. 3d–i, 4 and 5), (4) immunopositive for Glut (Glut +, Fig. 4), and (5) immunonegative for GABA, Gly or Glut (GABA-/Gly-/Glut- bouton). In the immunopositive boutons, gold particles were denser over vesicle clusters and mitochondria than over organelle-free areas. Gold particle densities for GABA in GABA + boutons and for Gly in Gly + boutons were 5.0–41.7 times

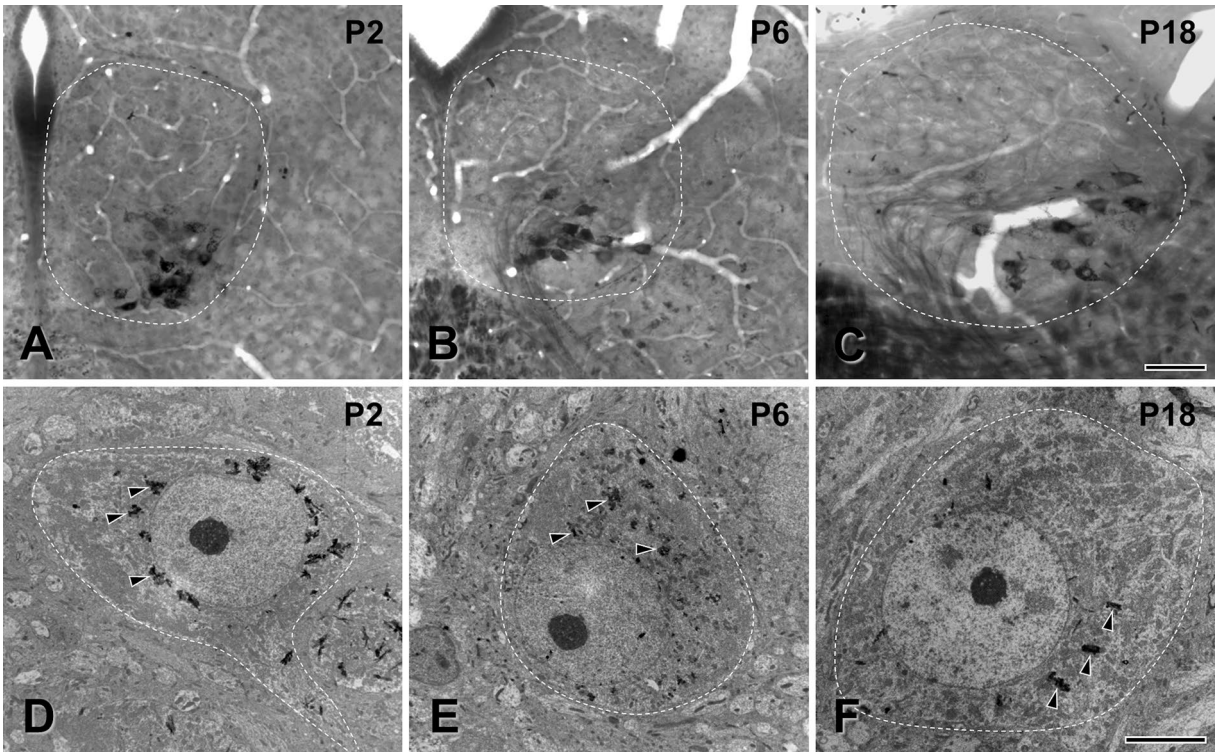

Fig. 1 Light (**a**–**c**) and electron (**d**–**f**) micrographs showing horseradish peroxidase (HRP)-labeled genioglossal (GG) motoneurons in the hypoglossal nucleus at postnatal days 2 (P2, **a**, **d**), 6 (P6, **b**, **e**) and 18 (P18, **c**, **f**). **a**–**c** HRP-labeled GG motoneurons in the ventral and ventrolateral regions of the hypoglossal nucleus. The GG motoneurons are small and close together at P2, and larger and farther apart at P18. **d**–**f** Retrogradely-transported HRP (arrowheads) in the somata of GG motoneurons. The hypoglossal nucleus in **a**–**c** and the somata of GG motoneurons in **d**–**f** are outlined with a dashed line. Scale bar = 100 μm in **c** (also applies to **a**, **b**); 5 μm in **f** (also applies to **d**, **e**)

and 5.0–31.7 times higher, respectively, than the respective background density (the density over the postsynaptic somatic compartment). Gold particle density for Glut was 1.1–27.5 times higher than the average tissue density + 2.576SD (Fig. 7).

The quantitative data on each of the immunopositive bouton types are presented in Table 2 and Figs. 6 and 7. Almost all (> 98%) boutons were immunopositive for GABA, Gly or Glut.

The number of GABA + only boutons decreased significantly; whereas those of Gly + only boutons and mixed GABA +/Gly + boutons increased significantly from P2/P6 to P18. The numbers of inhibitory boutons (GABA + and/or Gly + boutons) and excitatory boutons (Glut + boutons) increased significantly from P2 to P18 and from P2/P6 to P18, respectively.

The fractions of inhibitory and excitatory boutons of all boutons were not changed from P2 to P18. However, the fraction of inhibitory bouton types was significantly changed during postnatal development. Thus, the fraction of GABA + only boutons decreased significantly from P2 to P18; whereas that of Gly + only boutons increased significantly from P2/P6 to P18. The fraction of mixed GABA +/Gly + boutons increased significantly from P2 to P6/P18 and was the highest among all inhibitory bouton types from P2 to P18.

The mean lengths of bouton apposition, which is associated with bouton size, of mixed GABA +/Gly + boutons increased significantly from P2/P6 to P19; whereas those of GABA + only and Gly + only boutons was not significantly changed during postnatal development.

The synaptic covering percentage of GABA + only boutons decreased significantly, whereas those of Gly + only boutons and mixed GABA +/Gly + boutons increased significantly from P2/P6 to P18.

The packing density of GABA + only boutons decreased significantly from P2 to P18; whereas that of Gly + only boutons increased significantly from P2/P6 to P18. Those of mixed GABA +/Gly + boutons, inhibitory and excitatory boutons were not changed during postnatal development.

Discussion

The present study revealed that (1) the formation of new synapses onto the somata of rat GG motoneurons occurred primarily during the 2nd and 3rd postnatal weeks, (2) the

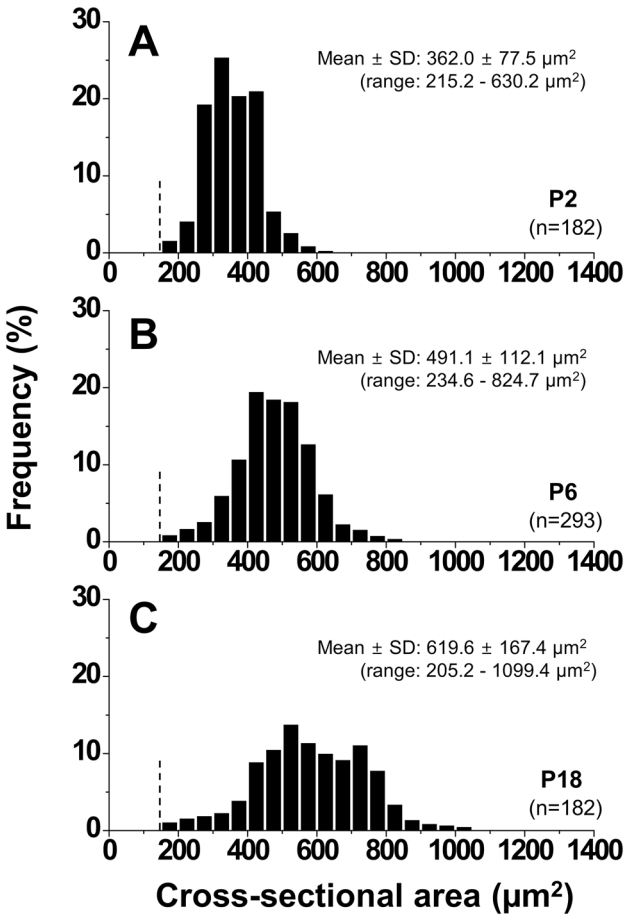

Fig. 2 Distribution of cross-sectional areas (μm^2) of somata of genioglossal motoneurons at postnatal days 2 (P2), P6 and P18. During development, large motoneurons become larger whereas small motoneurons remain unchanged. Dashed line is a reference for the cross-sectional area of the smallest somata at P2. "n =" is the total number of motoneurons measured at each age

Table 1 Quantitative data (mean ± SD) for boutons apposing somata of genioglossal motoneurons during postnatal development

Parameter	P2	P6	P18
Number of motoneurons examined	12	10	13
Number of boutons per motoneuron[1] (number of total boutons examined)	15.7 ± 4.2 (188)	18.5 ± 4.7 (185)	30.1 ± 8.5 (391)
Length of bouton apposition (μm)[1]	0.7 ± 0.1	0.8 ± 0.1	1.1 ± 0.1
Synaptic covering percentage (%)[1]	22.2 ± 4.9	26.8 ± 5.3	50.8 ± 12.8
Packing density	37.4 ± 8.2	31.4 ± 5.6	33.0 ± 10.5

[1]Indicates statistically significant difference between P2/P6 and P18 (one-way ANOVA, Scheffe's, $p < 0.05$)

number and fraction of GABA + only boutons decreased; whereas those of Gly + only boutons increased during the 2nd and 3rd postnatal weeks, and (3) the fraction of mixed GABA +/Gly + boutons of all boutons was consistently the highest among all inhibitory bouton types during the postnatal development.

The distinctive developmental pattern of inhibitory synapses onto the GG motoneurons may provide a window into understanding the mechanism of control of the precise and coordinated movements of the tongue during the maturation of the oral motor system.

Synapse formation and size of the GG motoneurons

The timeframe and rate of synapse formation during postnatal development are different in different regions and neuronal populations of the CNS (Vaughn 1989; Sanes et al. 2012). For example, the new synapse formation is dramatically increased during the first 10 postnatal days in the mouse olfactory bulb (Hinds and Hinds 1976) but during postnatal days 10–30 in the cat visual cortex (Cragg 1975). During the same timeframe, the process of new synapse formation is accompanied by a parallel process of synaptic pruning, by which inappropriately formed synapses are deleted (Hashimoto and Kano 2013; Vonhoff and Keshishian 2017). In the present study, the number of boutons on the somata of GG motoneurons increased dramatically during the 2nd and 3rd postnatal weeks, a critical period for the hypoglossal motoneuron development (Gao et al. 2011), and at variance with the time frame for synapse formation on the somata of the jaw-closing motoneurons (JC, P2–P31) and jaw-opening motoneurons (JO, P2–P11) (Paik et al. 2007,2012) which show dramatic increase of bouton number from neonatal period, even though all three classes are motoneurons of the oral motor system. Regulatory programs for myogenesis and synaptogenesis in tongue and masticatory muscles are different, which is thought to depend on their different embryonic origin, i.e., tongue muscle from somite and masticatory muscle from branchial arch (Yamane 2005). It is also possible to assume that the different time course for postnatal synapse formation between GG and masticatory motoneurons may be associated with different origin of their innervating muscles. Degenerative changes during early postnatal development, characteristic of boutons on somata of the spinal motoneurons (Ronnevi 1977, 1979), were not observed in boutons apposing GG motoneurons from P2 to P18, analogous to our findings in the JC and JO motoneurons (Paik et al. 2007, 2012). Given that the total number of synapses in the hypoglossal nucleus decreases after P20 (O'Kusky 1998), the process of pruning of synapses on the GG motoneuron somata likely begins after P18.

The fraction of Glut + boutons of all boutons on the GG motoneurons remained unchanged, but their mean length (a

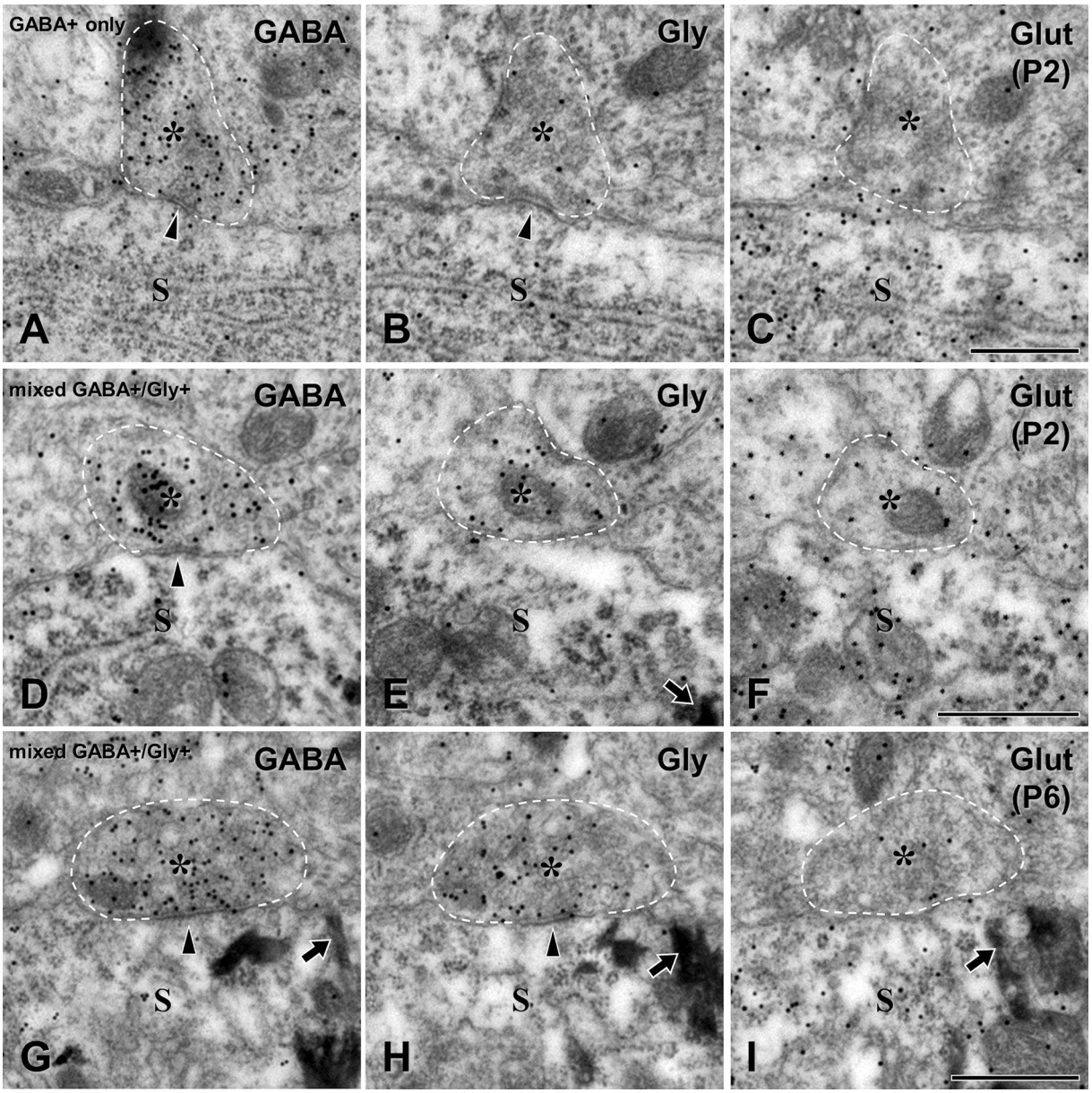

Fig. 3 Electron micrographs of adjacent thin sections incubated with antisera against GABA (**a**, **d**, **g**), glycine (Gly; **b**, **e**, **h**), and glutamate (Glut; **c**, **f**, **i**) showing boutons on somata (S) of genioglossal motoneurons at postnatal day 2 (P2; **a**–**f**) and P6 (**g**–**i**). Examples include boutons immunopositive for GABA alone (GABA + only bouton; **a**–**c**) and for both GABA and glycine (mixed GABA + /Gly + boutons; **d**–**f**, **g**–**i**). Boutons are outlined by a dashed line. Arrowheads indicate synapses. Arrows indicate retrogradely-transported HRP in somata of GG motoneurons. Scale bars = 500 nm in **c** (also applies to **a**, **b**), **f** (also applies to **d**, **e**) and **i** (also applies to **g**, **h**)

proxy for bouton size and, thus, synaptic strength) increased from P2 to P18, analogous to what we found about JC and JO motoneurons (Paik et al. 2012, 2011). The expression of various subunits of the postsynaptic Glut receptors in the hypoglossal nucleus changes during postnatal development (Whitney et al. 2000; Oshima et al. 2002; Wong-Riley and Liu 2005; Liu and Wong-Riley 2005, 2010), and so does the frequency of the presynaptic vesicular glutamate transporter 1 (VGLUT1)- and VGLUT2-immunopositive boutons (Pang et al. 2006). Given that the response of motoneurons to glutamate changes during early postnatal development (Gao et al. 2011; Nagata et al. 2016), the observation that the fraction of Glut + boutons of all boutons remains the same raises an assumption that the developmental change in the glutamatergic synaptic transmission onto the GG motoneurons may be due to changes in the functional properties of the pre- and/or postsynaptic elements of the synapse, rather than in their overall number. However, it should be also

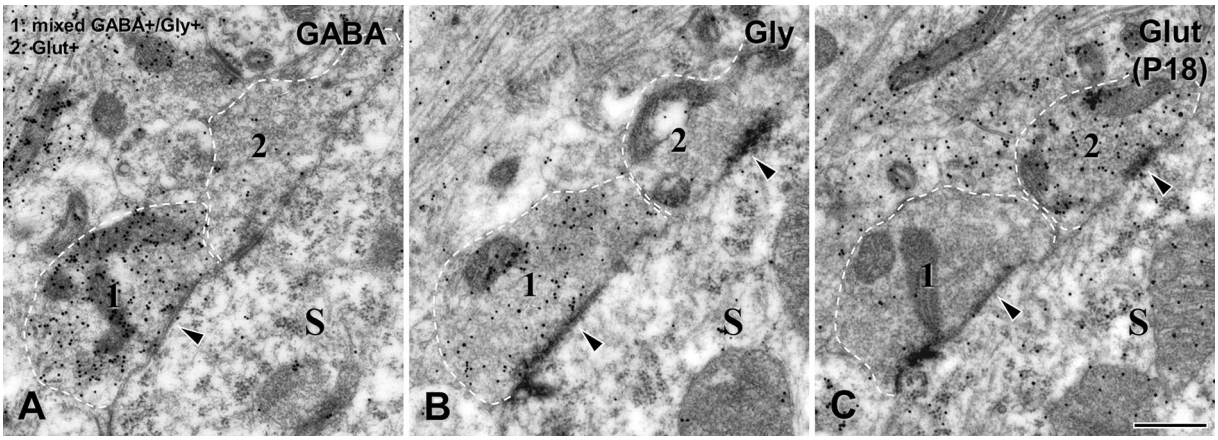

Fig. 4 Electron micrographs of adjacent thin sections incubated with antisera against GABA (**a**), glycine (**b**), and glutamate (**c**) on somata (S) of genioglossal motoneurons at postnatal day 18 (P18). Examples include boutons immunopositive for both GABA and glycine (mixed GABA + /Gly + bouton; "1") and immunonegative for both GABA and glycine but immunopositive for glutamate (Glut + bouton; "2"). Boutons are outlined by a dashed line. Arrowheads indicate synapses. Scale bar = 500 nm

noted that there is a limitation to understand glutamatergic transmission onto GG motoneurons by examining glutamatergic synapses only on their somata because vast majority of glutamatergic synapses are on dendrites and/or spines.

Inhibitory bouton types on the GG motoneurons during development

During the postnatal weeks 2 and 3, the number and the fraction of GABA + only boutons decreased by ~ 80% and ~ 90%; whereas at the same time, those of Gly + only boutons increased ~ 380% and ~ 260%, respectively. This corroborates the observation by Muller et al. (2006) of decreased density of GABA + puncta, and a concomitant increased density of Gly + puncta in the hypoglossal nucleus during postnatal development. The density of Gly receptor (GlyR) and the amplitude of glycinergic mIPSC also increased, and the density of $GABA_AR$ decreased (Muller et al. 2006, 2004). Taken together, these findings suggest that the inhibitory synapses on the GG motoneurons shift from GABAergic to glycinergic during postnatal development, consistent with the analogous switch in the spinal ventral horn and brain stem auditory nucleus (Gao et al. 2001; Nabekura et al. 2004).

That no degenerative changes were observed in GABA + only boutons suggests that the dramatic decrease of the number of GABA + only boutons from P6 to P18 is due to a switch to Gly + only boutons or mixed GABA + /Gly + boutons via an increase in the Gly content with or without a decrease of GABA content. Such switch of the neurotransmitter phenotype has been reported before, including stimulus-mediated neurotransmitter switch from dopaminergic to somatostatinergic in the hypothalamus (Dulcis et al. 2013; Meng et al. 2018), from noradrenergic to cholinergic for the sympathetic neurons (Habecker et al. 1995; Apostolova and Dechant 2009), etc. Since GABA and Gly are loaded into synaptic vesicles by the same vesicular inhibitory amino acid transporter (VIAAT) (Wojcik et al. 2006), a change in the uptake rate of VIAAT for cytosolic GABA or Gly (Aubrey 2016) can easily induce a phenotypic switch from GABA + boutons to Gly + or mixed GABA + /Gly + boutons during the postnatal development.

The fraction of mixed GABA + /Gly + boutons was the highest among inhibitory bouton types during postanal development

$GABA_AR$ and GlyR have different channel kinetics: GABAergic miniature inhibitory postsynaptic current (mIPSC) decays slowly; whereas, glycinergic mIPSC decays early and fast. In the present study, the mixed GABA + /Gly + boutons contained various ratios of GABA to Gly, analogous to some recent findings in the spinal cord, where the GABA/Gly co-releasing boutons invoke a large variety of mixed mIPSC (Aubrey and Supplisson 2018). This suggests that every mixed GABA + /Gly + bouton may release a different ratio of GABA to Gly thus contributing to the precise control of the timing of the GG motoneuron firing. The GG premotor neurons in the brain stem reticular formation project to JO and/or facial motoneurons, and are, thus, involved in the protrusion of the tongue and, at the same time, in jaw opening and/or lip lowering (Travers et al. 2005; Stanek et al. 2014). It is, thus, reasonable to assume that the majority of mixed GABA + /Gly + boutons on GG motoneurons arise from heterogenous premotor neurons and serve to fine tune the GG motoneuron inhibition that underlies the coordinated tongue movement during multiple oral behaviors.

The fraction of mixed GABA + /Gly + boutons was the highest among inhibitory bouton types during postnatal

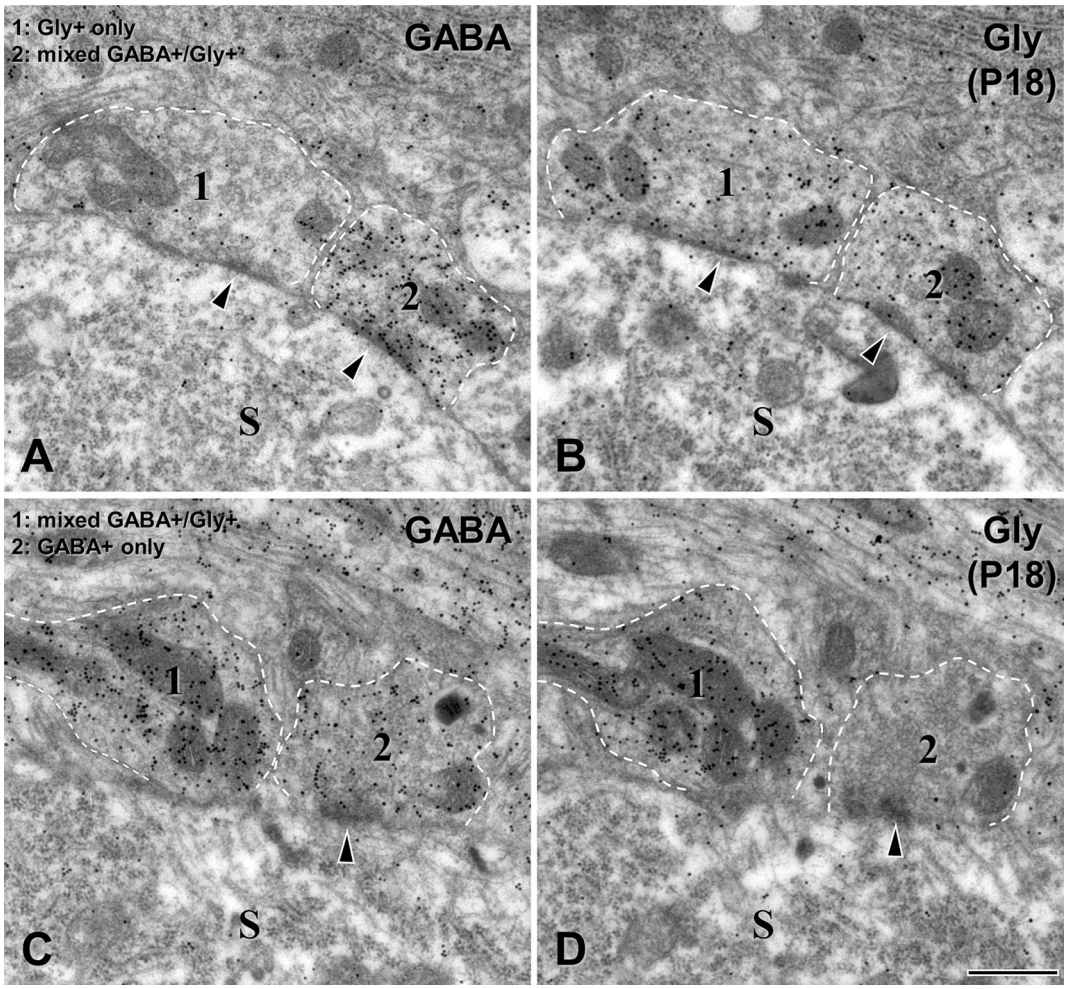

Fig. 5 Electron micrographs of adjacent thin sections incubated with antisera against GABA (**a**, **c**) and glycine (**b**, **d**) on the somata (S) of genioglossal motoneurons at postnatal day 18 (P18). Examples include a bouton immunopositive for glycine alone (Gly + only bouton, "1" in **a**, **b**), a bouton immunopositive for GABA alone (GABA + only bouton, "2" in **c**, **d**), and boutons immunopositive for both GABA and glycine (mixed GABA +/Gly + boutons, "2 in A, B, and "1" in **c**, **d**). Boutons are outlined by a dashed line. Arrowheads indicate synapses. Scale bar in **d** = 500 nm (also applies to **a**–**c**)

development, as well as in the adult (Paik et al. 2019). This is at variance with the electrophysiological finding that during postnatal development, the fraction of mixed mIPSC in the hypoglossal nucleus decreased and become inconspicuous; whereas that of the glycinergic mIPSC increased and become the most prominent among all mIPSC types (Muller et al. 2006; Gao et al. 2011). Other discrepancies involving presynaptic input from mixed GABA +/Gly + boutons include that only a small fraction of neurons that receive both GABAergic and glycinergic inputs exhibit mixed mIPSC (Inquimbert et al. 2007), and that although neurons in the anteroventral cochlear nucleus receive input from mixed GABA +/Gly + boutons, evoked IPSC are predominantly glycinergic (Lim et al. 2000). One way to reconcile these discrepancies is suggested by studies showing that, in the hypoglossal nucleus, spinal cord, and brain stem auditory nucleus, GABA in the mixed GABA +/Gly + boutons can act on presynaptic $GABA_AR$ and is, thus, involved in the feedback regulation of neurotransmitter release (Lim et al. 2000; Chery and Koninck 2000; O'Brien et al. 2004). At the same time, GABA released from mixed GABA +/Gly + boutons acts on postsynaptic GlyR to accelerate glycinergic transmission, shorten decay time of glycinergic mIPSC, and narrow the time window for effective inhibition (Lu et al. 2008). The precise regulation of glycinergic currents by GABA from mixed GABA +/Gly + boutons on the GG motoneurons made possible by this mechanism may be the basis for the precise regulation of the movements of the tongue in various oral behaviors.

Acknowledgments The authors sincerely thank Dr. Juli Valtschanoff for helpful discussion and careful reading of the manuscript. We also

Table 2 Quantitative data (mean ± SD) for GABA +, Gly + and Glut + boutons apposing somata of genioglossal motoneurons during postnatal development

Parameters	P2	P6	P18
Number of motoneurons examined	12	10	13
Number of total boutons examined	188	185	391
GABA + only boutons			
Total number of boutons	36	23	6
Number/motoneuron[1]	3.0 ± 1.2	2.3 ± 1.3	0.5 ± 0.5
Proportion of all bouton profiles (%)[2]	20.0 ± 7.5	12.5 ± 5.9	1.3 ± 1.5
Length of bouton apposition (μm)	0.7 ± 0.2	0.8 ± 0.3	0.8 ± 0.3
Synaptic covering percentage (%)[1]	3.8 ± 2.0	3.1 ± 2.2	0.4 ± 0.7
Packing density[2]	7.1 ± 2.7	4.0 ± 2.2	0.4 ± 0.7
Gly + only boutons			
Total number of boutons	10	9	44
Number/motoneuron[1]	0.8 ± 0.8	0.9 ± 1.0	3.4 ± 1.0
Proportion of all bouton profiles (%)[1]	5.5 ± 5.4	4.5 ± 5.0	11.5 ± 2.7
Length of bouton apposition (μm)	0.9 ± 0.3	0.8 ± 0.2	1.0 ± 0.3
Synaptic covering percentage (%)[1]	1.4 ± 1.3	1.4 ± 1.8	4.5 ± 3.3
Packing density[1]	1.6 ± 2.1	1.5 ± 1.4	3.7 ± 1.7
Mixed GABA +/Gly + boutons			
Total number of boutons	41	60	132
Number/motoneuron[1]	3.4 ± 1.8	6.0 ± 1.8	10.2 ± 4.9
Proportion of all bouton profiles (%)[3]	21.3 ± 7.3	33.1 ± 8.4	32.6 ± 8.2
Length of bouton apposition (μm)[1]	0.7 ± 0.1	0.8 ± 0.2	1.1 ± 0.2
Synaptic covering percentage (%)[1]	4.8 ± 2.1	9.3 ± 3.2	17.4 ± 9.9
Packing density	8.2 ± 3.9	11.1 ± 4.5	11.7 ± 5.1
GABA + and/or Gly + boutons			
Total number of boutons	87	92	182
Number/motoneuron[4]	7.3 ± 2.5	9.2 ± 3.0	14.0 ± 5.8
Proportion of all bouton profiles (%)	46.7 ± 9.7	50.1 ± 12.5	45.4 ± 8.0
Length of bouton apposition (μm)[1]	0.7 ± 0.1	0.8 ± 0.2	1.0 ± 0.2
Synaptic covering percentage (%)[1]	10.0 ± 3.3	13.6 ± 5.3	22.3 ± 11.4
Packing density	16.0 ± 4.3	15.1 ± 5.2	16.2 ± 6.8
Glut + boutons			
Total number of boutons	99	91	207
Number/motoneuron[1]	8.3 ± 2.8	9.1 ± 3.4	15.9 ± 3.9
Proportion of all bouton profiles (%)	52.2 ± 10.1	49.1 ± 12.5	54.2 ± 8.1
Length of bouton apposition (μm)[2]	0.7 ± 0.1	0.8 ± 0.1	1.2 ± 0.2
Synaptic covering percentage (%)[1]	11.8 ± 4.0	12.9 ± 3.5	27.9 ± 3.8
Packing density	20.9 ± 8.3	15.6 ± 5.1	17.0 ± 5.9
GABA −/Gly −/Glut − boutons			
Total number of boutons	2	2	2
Number/motoneuron	0.2 ± 0.4	0.2 ± 0.4	0.2 ± 0.4
Proportion of all bouton profiles (%)	1.1 ± 2.5	0.8 ± 1.7	0.4 ± 1.1
Length of bouton apposition (μm)[1]	0.8 ± 0.2	0.8 ± 0.2	1.1 ± 0.3
Synaptic covering percentage (%)	0.6 ± 0.9	0.2 ± 0.5	0.5 ± 1.1
Packing density	0.6 ± 1.1	0.3 ± 0.8	0.3 ± 0.7

[1]Indicates statistically significant difference between P2/P6 and P18 (one-way ANOVA, Scheffe's, $p < 0.05$)

[2]Indicates statistically significant difference among P2, P6 and P18 (one-way ANOVA, Scheffe's, $p < 0.05$)

[3]Indicates statistically significant difference between P2 and P6/P18 (one-way ANOVA, Scheffe's, $p < 0.05$)

[4]Indicates statistically significant difference between P2 and P18 (one-way ANOVA, Scheffe's, $p < 0.05$)

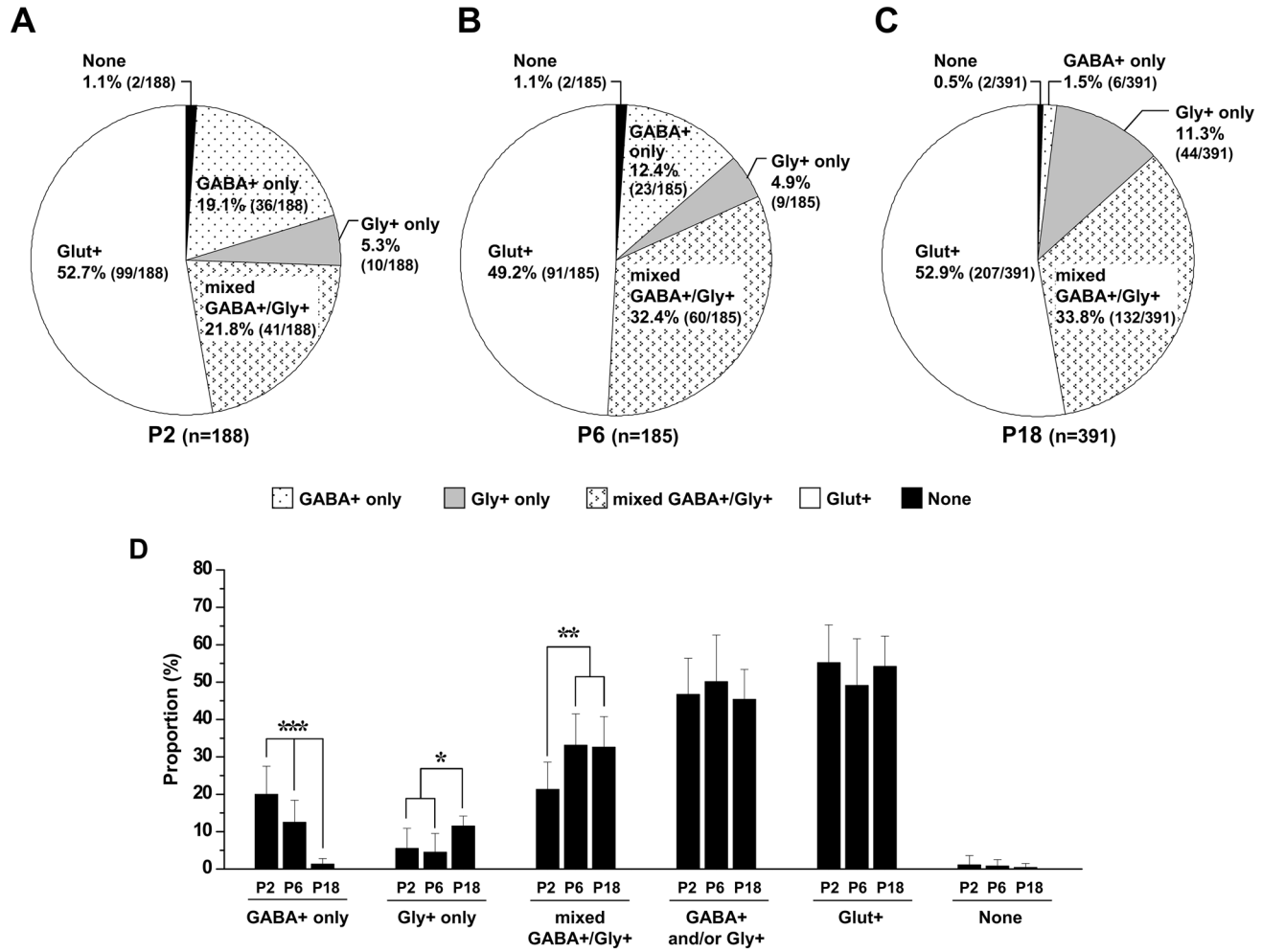

Fig. 6 Distribution of excitatory and inhibitory boutons apposing somata of genioglossal (GG) motoneurons at different stages of postnatal development. **a**–**c** Percentages of each immunopositive bouton type of all boutons. "None" indicates boutons immunonegative for GABA, glycine, or glutamate. **d** Mean ± SD of each immunopositive bouton type. "GABA + and/or Gly +" indicates the sum of all inhibitory boutons. ***$p < 0.001$; **$p < 0.01$; *$p < 0.05$ (one-way ANOVA, Scheffe's test)

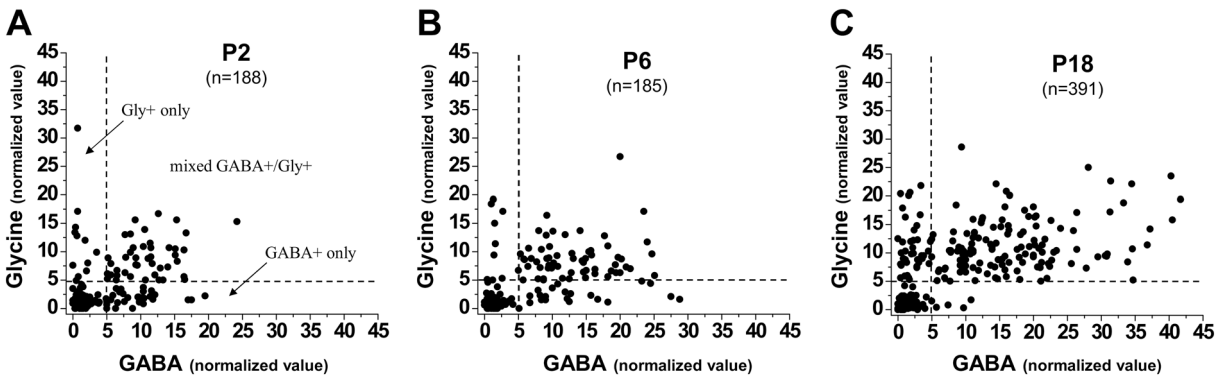

Fig. 7 Scatterplots of the normalized values of gold particle density relative to background density (gold particle density in bouton/background density) for GABA (abscissa) and glycine (ordinate) in boutons apposing somata of genioglossal (GG) motoneurons at postnatal days 2 (P2: **a**), P6 (**b**), and P18 (**c**). A bouton was considered immunopositive when the gold particle density over vesicle areas of the bouton was five times (dashed line) higher than the background density (gold particle density in the cytoplasm of the postsynaptic neurons). Note that the mixed GABA +/Gly + boutons have different ratios of GABA to glycine. A dot indicates a bouton apposing somata of GG motoneuron

sincerely thank Dr. O.P. Ottersen for the gift of the glutamate, GABA and glycine antibodies and the sandwich block for the test sections.

Funding This work was supported by the National Research Foundation of Korea (NRF) grant funded by the Korea government (MSIT, NRF-2017R1A5A2015391, NRF-2017R1A2B2003561).

Compliance with ethical standards

Conflict of interest The authors declare that they have no conflict of interest.

Ethics approval All applicable international, national, and/or institutional guidelines for the care and use of animals were followed. All procedures performed in studies involving animals were in accordance with the ethical standards of the institution or practice at which the studies were conducted.

References

Apostolova G, Dechant G (2009) Development of neurotransmitter phenotypes in sympathetic neurons. Auton Neurosci 151:30–38. https://doi.org/10.1016/j.autneu.2009.08.012

Aubrey KR (2016) Presynaptic control of inhibitory neurotransmitter content in VIAAT containing synaptic vesicles. Neurochem Int 98:94–102. https://doi.org/10.1016/j.neuint.2016.06.002

Aubrey KR, Supplisson S (2018) Heterogeneous signaling at GABA and glycine co-releasing terminals. Front Synaptic Neurosci 10:40. https://doi.org/10.3389/fnsyn.2018.00040

Bae JY, Lee JS, Ko SJ, Cho YS, Rah JC, Cho HJ, Park MJ, Bae YC (2018) Extrasynaptic homomeric glycine receptors in neurons of the rat trigeminal mesencephalic nucleus. Brain Struct Funct 223:2259–2268. https://doi.org/10.1007/s00429-018-1607-3

Berger AJ (2011) Development of synaptic transmission to respiratory motoneurons. Respir Physiol Neurobiol 179:34–42. https://doi.org/10.1016/j.resp.2011.03.002

Broman J, Anderson S, Ottersen OP (1993) Enrichment of glutamate-like immunoreactivity in primary afferent terminals throughout the spinal cord dorsal horn. Eur J Neurosci 5:1050–1061. https://doi.org/10.1111/j.1460-9568.1993.tb00958.x

Carrascal L, Nieto-Gonzalez JL, Cameron WE, Torres B, Nunez-Abades PA (2005) Changes during the postnatal development in physiological and anatomical characteristics of rat motoneurons studied in vitro. Brain Res Brain Res Rev 49:377–387. https://doi.org/10.1016/j.brainresrev.2005.02.003

Chery N, De Koninck Y (2000) GABA(B) receptors are the first target of released GABA at lamina I inhibitory synapses in the adult rat spinal cord. J Neurophysiol 84:1006–1011. https://doi.org/10.1152/jn.2000.84.2.1006

Cragg BG (1975) The development of synapses in the visual system of the cat. J Comp Neurol 160:147–166. https://doi.org/10.1002/cne.901600202

Dulcis D, Jamshidi P, Leutgeb S, Spitzer NC (2013) Neurotransmitter switching in the adult brain regulates behavior. Science 340:449–453. https://doi.org/10.1126/science.1234152

Gao BX, Stricker C, Ziskind-Conhaim L (2001) Transition from GABAergic to glycinergic synaptic transmission in newly formed spinal networks. J Neurophysiol 86:492–502. https://doi.org/10.1152/jn.2001.86.1.492

Gao XP, Liu QS, Liu Q, Wong-Riley MT (2011) Excitatory-inhibitory imbalance in hypoglossal neurons during the critical period of postnatal development in the rat. J Physiol 589:1991–2006. https://doi.org/10.1113/jphysiol.2010.198945

Habecker BA, Tresser SJ, Rao MS, Landis SC (1995) Production of sweat gland cholinergic differentiation factor depends on innervation. Dev Biol 167:307–316. https://doi.org/10.1006/dbio.1995.1025

Hashimoto K, Kano M (2013) Synapse elimination in the developing cerebellum. Cell Mol Life Sci 70:4667–4680. https://doi.org/10.1007/s00018-013-1405-2

Hinds JW, Hinds PL (1976) Synapse formation in the mouse olfactory bulb. I. Quantitative studies. J Comp Neurol 169:15–40. https://doi.org/10.1002/cne.901690103

Horner RL (2009) Emerging principles and neural substrates underlying tonic sleep-state-dependent influences on respiratory motor activity. Philos Trans R Soc Lond B Biol Sci 364:2553–2564. https://doi.org/10.1098/rstb.2009.0065

Inquimbert P, Rodeau JL, Schlichter R (2007) Differential contribution of GABAergic and glycinergic components to inhibitory synaptic transmission in lamina II and laminae III–IV of the young rat spinal cord. Eur J Neurosci 26:2940–2949. https://doi.org/10.1111/j.1460-9568.2007.05919.x

Kolston J, Osen KK, Hackney CM, Ottersen OP, Storm-Mathisen J (1992) An atlas of glycine- and GABA-like immunoreactivity and colocalization in the cochlear nuclear complex of the guinea pig. Anat Embryol (Berl) 186:443–465

Lim R, Alvarez FJ, Walmsley B (2000) GABA mediates presynaptic inhibition at glycinergic synapses in a rat auditory brainstem nucleus. J Physiol 525(Pt 2):447–459. https://doi.org/10.1111/j.1469-7793.2000.t01-1-00447.x

Liu Q, Wong-Riley MT (2005) Postnatal developmental expressions of neurotransmitters and receptors in various brain stem nuclei of rats. J Appl Physiol 98:1442–1457. https://doi.org/10.1152/japplphysiol.01301.2004

Liu Q, Wong-Riley MT (2010) Postnatal development of *N*-methyl-D-aspartate receptor subunits 2A, 2B, 2C, 2D, and 3B immunoreactivity in brain stem respiratory nuclei of the rat. Neuroscience 171:637–654. https://doi.org/10.1016/j.neuroscience.2010.09.055

Liu X, Sood S, Liu H, Nolan P, Morrison JL, Horner RL (2003) Suppression of genioglossus muscle tone and activity during reflex hypercapnic stimulation by GABA(A) mechanisms at the hypoglossal motor nucleus in vivo. Neuroscience 116:249–259

Lu T, Rubio ME, Trussell LO (2008) Glycinergic transmission shaped by the corelease of GABA in a mammalian auditory synapse. Neuron 57:524–535. https://doi.org/10.1016/j.neuron.2007.12.010

Meng D, Li HQ, Deisseroth K, Leutgeb S, Spitzer NC (2018) Neuronal activity regulates neurotransmitter switching in the adult brain following light-induced stress. Proc Natl Acad Sci USA 115:5064–5071. https://doi.org/10.1073/pnas.1801598115

Muller E, Triller A, Legendre P (2004) Glycine receptors and GABA receptor alpha 1 and gamma 2 subunits during the development of mouse hypoglossal nucleus. Eur J Neurosci 20:3286–3300. https://doi.org/10.1111/j.1460-9568.2004.03785.x

Muller E, Le Corronc H, Triller A, Legendre P (2006) Developmental dissociation of presynaptic inhibitory neurotransmitter and postsynaptic receptor clustering in the hypoglossal nucleus. Mol Cell Neurosci 32:254–273. https://doi.org/10.1016/j.mcn.2006.04.007

Nabekura J, Katsurabayashi S, Kakazu Y, Shibata S, Matsubara A, Jinno S, Mizoguchi Y, Sasaki A, Ishibashi H (2004) Developmental switch from GABA to glycine release in single central synaptic terminals. Nat Neurosci 7:17–23. https://doi.org/10.1038/nn1170

Nagata S, Nakamura S, Nakayama K, Mochizuki A, Yamamoto M, Inoue T (2016) Postnatal changes in glutamatergic inputs of jaw-closing motoneuron dendrites. Brain Res Bull 127:47–55. https://doi.org/10.1016/j.brainresbull.2016.08.014

O'Brien JA, Berger AJ (2001) The nonuniform distribution of the GABA(A) receptor alpha 1 subunit influences inhibitory synaptic

transmission to motoneurons within a motor nucleus. J Neurosci 21:8482–8494
O'Brien JA, Sebe JY, Berger AJ (2004) GABA(B) modulation of GABA(A) and glycine receptor-mediated synaptic currents in hypoglossal motoneurons. Respir Physiol Neurobiol 141:35–45. https://doi.org/10.1016/j.resp.2004.03.009
O'Kusky JR (1998) Postnatal changes in the numerical density and total number of asymmetric and symmetric synapses in the hypoglossal nucleus of the rat. Brain Res Dev Brain Res 108:179–191. https://doi.org/10.1016/s0165-3806(98)00048-0
Oshima S, Fukaya M, Masabumi N, Shirakawa T, Oguchi H, Watanabe M (2002) Early onset of NMDA receptor GluR epsilon 1 (NR2A) expression and its abundant postsynaptic localization in developing motoneurons of the mouse hypoglossal nucleus. Neurosci Res 43:239–250. https://doi.org/10.1016/s0168-0102(02)00035-4
Ottersen OP, Storm-Mathisen J (1984) Glutamate- and GABA-containing neurons in the mouse and rat brain, as demonstrated with a new immunocytochemical technique. J Comp Neurol 229:374–392. https://doi.org/10.1002/cne.902290308
Ottersen OP, Storm-Mathisen J, Madsen S, Skumlien S, Stromhaug J (1986) Evaluation of the immunocytochemical method for amino acids. Med Biol 64:147–158
Paik SK, Bae JY, Park SE, Moritani M, Yoshida A, Yeo EJ, Choi KS, Ahn DK, Moon C, Shigenaga Y, Bae YC (2007) Developmental changes in distribution of gamma-aminobutyric acid- and glycine-immunoreactive boutons on rat trigeminal motoneurons. I. Jaw-closing motoneurons. J Comp Neurol 503:779–789. https://doi.org/10.1002/cne.21423
Paik SK, Park SK, Jin JK, Bae JY, Choi SJ, Yoshida A, Ahn DK, Bae YC (2011) Ultrastructural analysis of glutamate-immunopositive synapses onto the rat jaw-closing motoneurons during postnatal development. J Neurosci Res 89:153–161. https://doi.org/10.1002/jnr.22544
Paik SK, Kwak WK, Bae JY, Na YK, Park SY, Yi HW, Ahn DK, Ottersen OP, Yoshida A, Bae YC (2012) Development of gamma-aminobutyric acid-, glycine-, and glutamate-immunopositive boutons on rat jaw-opening motoneurons. J Comp Neurol 520:1212–1226. https://doi.org/10.1002/cne.22771
Paik SK, Yoo HI, Choi SK, Bae JY, Park SK, Bae YC (2019) Distribution of excitatory and inhibitory axon terminals on the rat hypoglossal motoneurons. Brain Struct Funct 224:1767–1779. https://doi.org/10.1007/s00429-019-01874-0
Pang YW, Li JL, Nakamura K, Wu S, Kaneko T, Mizuno N (2006) Expression of vesicular glutamate transporter 1 immunoreactivity in peripheral and central endings of trigeminal mesencephalic nucleus neurons in the rat. J Comp Neurol 498:129–141. https://doi.org/10.1002/cne.21047
Park SK, Lee DS, Bae JY, Bae YC (2016) Central connectivity of the chorda tympani afferent terminals in the rat rostral nucleus of the solitary tract. Brain Struct Funct 221:1125–1137. https://doi.org/10.1007/s00429-014-0959-6
Park SK, Ko SJ, Paik SK, Rah JC, Lee KJ, Bae YC (2018) Vesicular glutamate transporter 1 (VGLUT1)- and VGLUT2-immunopositive axon terminals on the rat jaw-closing and jaw-opening motoneurons. Brain Struct Funct 223:2323–2334. https://doi.org/10.1007/s00429-018-1636-y
Park SK, Hong JH, Jung JK, Ko HG, Bae YC (2019a) Vesicular Glutamate Transporter 1 (VGLUT1)- and VGLUT2-containing terminals on the rat jaw-closing gamma-motoneurons. Exp Neurobiol 28:451–457. https://doi.org/10.5607/en.2019.28.4.451
Park SK, Devi AP, Bae JY, Cho YS, Ko HG, Kim DY, Bae YC (2019b) Synaptic connectivity of urinary bladder afferents in the rat superficial dorsal horn and spinal parasympathetic nucleus. J Comp Neurol 527:3002–3013. https://doi.org/10.1002/cne.24725
Plowman L, Lauff DC, Berthon-Jones M, Sullivan CE (1990) Waking and genioglossus muscle responses to upper airway pressure oscillation in sleeping dogs. J Appl Physiol 68:2564–2573. https://doi.org/10.1152/jappl.1990.68.6.2564
Ronnevi LO (1977) Spontaneous phagocytosis of boutons on spinal motoneurons during early postnatal development. An electron microscopical study in the cat. J Neurocytol 6:487–504. https://doi.org/10.1007/BF01205215
Ronnevi LO (1979) Spontaneous phagocytosis of C-type synaptic terminals by spinal alpha-motoneurons in newborn kittens. An electron microscopic study. Brain Res 162:189–199. https://doi.org/10.1016/0006-8993(79)90283-x
Sanes DH, Reh TA, Harris WA (2012) Synapse formation and function. In: Sanes DH, Reh TA, Harris WA (eds) Development of the nervous system, 3rd edn. Elsevier, Amsterdam, pp 209–248
Singer JH, Berger AJ (2000) Development of inhibitory synaptic transmission to motoneurons. Brain Res Bull 53:553–560
Stanek E 4th, Cheng S, Takatoh J, Han BX, Wang F (2014) Monosynaptic premotor circuit tracing reveals neural substrates for oro-motor coordination. Elife 3:e02511. https://doi.org/10.7554/eLife.02511
Travers JB, Yoo JE, Chandran R, Herman K, Travers SP (2005) Neurotransmitter phenotypes of intermediate zone reticular formation projections to the motor trigeminal and hypoglossal nuclei in the rat. J Comp Neurol 488:28–47. https://doi.org/10.1002/cne.20604
Vaughn JE (1989) Fine structure of synaptogenesis in the vertebrate central nervous system. Synapse 3:255–285. https://doi.org/10.1002/syn.890030312
Vonhoff F, Keshishian H (2017) Activity-dependent synaptic refinement: new insights from Drosophila. Front Syst Neurosci 11:23. https://doi.org/10.3389/fnsys.2017.00023
Weinberg RJ, van Eyck SL (1991) A tetramethylbenzidine/tungstate reaction for horseradish peroxidase histochemistry. J Histochem Cytochem 39:1143–1148. https://doi.org/10.1177/39.8.1906909
Whitney GM, Ohtake PJ, Simakajornboon N, Xue YD, Gozal D (2000) AMPA glutamate receptors and respiratory control in the developing rat: anatomic and pharmacological aspects. Am J Physiol Regul Integr Comp Physiol 278:R520-528. https://doi.org/10.1152/ajpregu.2000.278.2.R520
Wojcik SM, Katsurabayashi S, Guillemin I, Friauf E, Rosenmund C, Brose N, Rhee JS (2006) A shared vesicular carrier allows synaptic corelease of GABA and glycine. Neuron 50:575–587. https://doi.org/10.1016/j.neuron.2006.04.016
Wong-Riley MT, Liu Q (2005) Neurochemical development of brain stem nuclei involved in the control of respiration. Respir Physiol Neurobiol 149:83–98. https://doi.org/10.1016/j.resp.2005.01.011
Yamane A (2005) Embryonic and postnatal development of masticatory and tongue muscles. Cell Tissue Res 322:183–189. https://doi.org/10.1007/s00441-005-0019-x